

# PSR J1740–3052 — a pulsar with a massive companion

I. H. Stairs,<sup>1,2</sup> R. N. Manchester,<sup>3</sup> A. G. Lyne,<sup>1</sup> V. M. Kaspi,<sup>4\*</sup> F. Camilo,<sup>5</sup> J. F. Bell,<sup>3</sup> N. D’Amico,<sup>6,7</sup> M. Kramer,<sup>1</sup> F. Crawford,<sup>8†</sup>, D. J. Morris,<sup>1</sup> A. Possenti,<sup>6</sup> N. P. F. McKay,<sup>1</sup> S. L. Lumsden,<sup>9</sup> L. E. Tacconi-Garman,<sup>10</sup> R. D. Cannon,<sup>11</sup> N. C. Hambly,<sup>12</sup> P. R. Wood<sup>13</sup>

<sup>1</sup>University of Manchester, Jodrell Bank Observatory, Macclesfield, Cheshire, SK11 9DL, UK

<sup>2</sup>National Radio Astronomy Observatory, P.O. Box 2, Green Bank, WV 24944, USA; email: [istairs@nrao.edu](mailto:istairs@nrao.edu)

<sup>3</sup>Australia Telescope National Facility, CSIRO, P.O. Box 76, Epping NSW 1710, Australia

<sup>4</sup>Physics Department, McGill University, 3600 University Street, Montreal, Quebec, H3A 2T8, Canada

<sup>5</sup>Columbia Astrophysics Laboratory, Columbia University, 550 W. 120th Street, New York, NY 10027, USA

<sup>6</sup>Osservatorio Astronomico di Bologna, via Ranzani 1, 40127 Bologna, Italy

<sup>7</sup>Instituto di Radioastronomia del CNR, via Gobetti 101, 40129 Bologna, Italy

<sup>8</sup>Massachusetts Institute of Technology, Center for Space Research, 70 Vassar Street, Cambridge, MA 02139, USA

<sup>9</sup>Department of Physics and Astronomy, E. C. Stoner Building, University of Leeds, Leeds, W. Yorkshire, L52 9JT, UK

<sup>10</sup>Max-Planck-Institut für Extraterrestrische Physik, Postfach 1312, 85741 Garching, Germany

<sup>11</sup>Anglo-Australian Observatory, P.O. Box 296, Epping NSW 1710, Australia

<sup>12</sup>Institute for Astronomy, University of Edinburgh, Royal Observatory, Blackford Hill, Edinburgh, EH9 3HJ, UK

<sup>13</sup>Research School of Astronomy & Astrophysics, Institute of Advanced Studies, The Australian National University, Cotter Road, Weston Creek, ACT 2611, Australia

28 August 2021

## ABSTRACT

We report on the discovery of a binary pulsar, PSR J1740–3052, during the Parkes multibeam survey. Timing observations of the 570-ms pulsar at Jodrell Bank and Parkes show that it is young, with a characteristic age of 350 kyr, and is in a 231-day, highly eccentric orbit with a companion whose mass exceeds  $11 M_{\odot}$ . An accurate position for the pulsar was obtained using the Australia Telescope Compact Array. Near-infrared 2.2- $\mu$ m observations

make with the telescopes at the Siding Spring observatory reveal a late-type star coincident with the pulsar position. However, we do not believe that this star is the pulsar's companion, because a typical star of this spectral type and required mass would extend beyond the pulsar's orbit. Furthermore, the measured advance of periastron of the pulsar suggests a more compact companion, for example, a main-sequence star with radius only a few times that of the sun. Such a companion is also more consistent with the small dispersion measure variations seen near periastron. Although we cannot conclusively rule out a black-hole companion, we believe the companion is probably an early B star, making the system similar to the binary PSR J0045–7319.

**Key words:** pulsars: general — pulsars: individual (PSR J1740–3052) — binaries: general — stars: late-type — stars: mass loss — X-rays: stars

## 1 INTRODUCTION

Radio pulsars in binary systems provide a wealth of information about neutron stars, their companions, and binary evolution. Through radio and optical observations of double-neutron-star and neutron-star–white-dwarf binaries, an overall picture of binary pulsar evolution has emerged (see, e.g., Bhattacharya and van den Heuvel 1991 and Phinney and Kulkarni 1994). Young pulsars lose energy in the form of particles or electromagnetic waves and are believed to spin down with approximately constant magnetic field, eventually reaching the point at which the radio emission mechanism is no longer effective. An isolated neutron star will never again be observed as a radio pulsar. However, a neutron star with a non-degenerate companion may be ‘recycled’ by accreting mass and orbital angular momentum from the evolving companion in an X-ray binary phase. The pulsar's spin period is decreased, its magnetic field is reduced, and it begins once more to emit as a radio pulsar. There are several possible branches to this evolution. Low-mass companions permit stable mass transfer to the neutron star over the lifetime of the giant phase, resulting in pulsars with spin periods of a few milliseconds and low-mass He white-dwarf companions. Unstable mass transfer from higher-mass red giants may yield pulsars with slightly longer spin periods and heavier, CO white-dwarf companions. A companion massive enough to undergo a

\* On leave from Massachusetts Institute of Technology, Center for Space Research, 70 Vassar Street, Cambridge, MA 02139, USA

† Present address: Management and Data Systems Division, Lockheed Martin Corporation, P.O. Box 8048, Philadelphia, PA 19101, USA

supernova explosion itself will result in either an unbound pair of neutron stars, one somewhat recycled, one young, or a double-neutron-star system such as PSR B1913+16 (Hulse & Taylor 1975).

The precursors to these evolved binary systems must be young neutron stars with non-degenerate companions, and some of these neutron stars should be visible as radio pulsars. Indeed, two such objects have been reported to date: PSR B1259–63, with a  $\sim 10 M_{\odot}$  Be-star companion (Johnston et al. 1992), and PSR J0045–7319, whose companion is a B star also of mass  $\sim 10 M_{\odot}$  (Kaspi et al. 1994). Both of these main-sequence binaries are believed to be progenitors of high-mass X-ray binaries (HMXBs).

In this paper, we report on the discovery of a third young radio pulsar with a massive companion. PSR J1740–3052 is a 570 ms pulsar which is in a 231-day binary orbit with a companion of minimum mass  $11 M_{\odot}$ . This pulsar was discovered in the ongoing Parkes multibeam pulsar survey, a large-scale survey for pulsars currently being carried out using the 13-beam 1400-MHz receiver on the Parkes 64-m radio telescope of the Australia Telescope National Facility (Manchester et al. 2001). The discovery observations, radio pulse timing and interferometric observations, and the results obtained from them are described in §2. Near-infrared observations made to identify the pulsar companion are described in §3. Radio and X-ray observations made around periastron passages are described in §4. In §5 we discuss the implications of the observational results and the nature of the pulsar companion.

## 2 RADIO OBSERVATIONS AND TIMING SOLUTION

### 2.1 Observations and Data Reduction

PSR J1740–3052 was initially observed on 1997 Aug. 25, and the survey reduction software identified it as a candidate with a 570-ms period and dispersion measure (DM) of  $739 \text{ cm}^{-3} \text{ pc}$ . Survey parameters and procedures are described in detail by Manchester et al. (2001). The confirmation observation gave a period which was substantially different from the initial discovery period, indicating possible membership of a binary system. The pulsar has since been observed in a series of timing measurements at both the Parkes 64-m telescope and the Lovell 76-m telescope at Jodrell Bank Observatory, UK.

At Parkes, most data are recorded using the central beam of the multibeam system, with a  $2 \times 96 \times 3$  MHz filterbank centred on 1374 MHz and a digital sampling rate of  $250 \mu\text{s}$ . Details of the timing observations may be found in Manchester et al. (2001). The pulsar is

also frequently observed at 660 MHz, using a filterbank consisting of  $2 \times 256 \times 0.125$  MHz channels.

Observations at Jodrell Bank are made in a band centred near 1400 MHz. The filterbank consisted of  $2 \times 32 \times 3$  MHz channels centred on 1376 MHz until 1999 Aug., and  $2 \times 64 \times 1$  MHz channels centred on 1396 MHz thereafter.

Data from both Parkes and Jodrell Bank are de-dispersed and folded at the predicted topocentric pulsar period. This process is performed offline for the Parkes data and online for the Jodrell Bank data. Total integration times per observation were typically 10 min at Parkes and 30 min at Jodrell Bank. Each pulse profile obtained by summing over an observation is convolved with a high signal-to-noise ratio “standard profile” producing a topocentric time-of-arrival (TOA). These are then processed using the TEMPO program<sup>‡</sup>. Barycentric corrections are obtained using the Jet Propulsion Laboratory DE200 solar-system ephemeris (Standish 1982). The standard profiles at the two observing frequencies are shown in Fig. 1.

## 2.2 Interferometric Position Determination

As PSR J1740–3052 lies close to the ecliptic and is a member of a long-period binary system, its position cannot yet be well determined through standard pulsar timing analyses. We therefore undertook observations with the 6-element Australia Telescope Compact Array (ATCA) on 1999 April 20. Pulsar gating mode was used for simultaneous observations at frequencies of 1384 MHz and 2496 MHz, with 128 MHz bandwidth in both polarisations at each frequency. The source 1934–638 was used to give the primary flux density calibration and the three sources 1714–252, 1751–253 and 1830–360 were used as phase calibrators. The MIRIAD software package<sup>§</sup> was used to produce on- and off-pulse images of the pulsar field, and to fit a point source to the differenced image. These images were made separately using each of the phase calibrators at each of the two frequencies, yielding five semi-independent determinations of the position (the calibration source 1830–360 was resolved for long baselines at 2496 MHz and therefore was not usable at this frequency) from which the position and its uncertainty were derived. This position is listed in Table 1. In these and other entries in this table, the uncertainty is given in parentheses and refers to the last quoted digit.

<sup>‡</sup> See <http://pulsar.princeton.edu/tempo>.

<sup>§</sup> See <http://www.atnf.csiro.au/computing/software/miriad>.

### 2.3 Timing Results and Implications

Continued timing observations at Jodrell Bank and Parkes confirmed that PSR J1740–3052 is a member of a binary system in a highly eccentric orbit. Fig. 2 shows the measured period variation of PSR J1740–3052 through the orbital period of 231 days. Subsequently, we performed a phase-coherent analysis of the arrival times over the period 1998 Aug. 7 – 2000 Nov. 23, using the main-sequence-star binary model of Wex (1998) in TEMPO. The results are summarized in Table 1. The errors are twice the formal  $1\sigma$  values from the TEMPO solution; we consider these to be conservative estimates of the true  $1\sigma$  errors. Timing residuals are shown in Fig. 3. The DM was obtained using the 1400 MHz observations and five 660 MHz observations at orbital phases far from periastron. Uncertainties in the pulse arrival times were determined by requiring that the reduced  $\chi^2$  be 1.0 for the individual data sets from the different receivers and telescopes. There are clearly some remaining systematic trends in the residuals. As the orbital period is roughly 8 months and the sampling is irregular, we are not yet able to fully distinguish between orbital and annual effects in the data. For this reason, we have fixed the position at that determined by the ATCA observations, and find, in the best simultaneous fit of all parameters, a marginally significant result for the advance of periastron,  $\dot{\omega}$ . If  $\dot{\omega}$  is not included in the fit, the overall reduced  $\chi^2$  increases from 1.05 to 1.20; this increases our confidence in the significance of the parameter. With continued long-term timing, it should be possible to refine the position as well as  $\dot{\omega}$  and other orbital parameters such as the change in projected semi-major axis,  $\dot{x}$ , and the orbital period derivative,  $\dot{P}_b$ .

The spin parameters for PSR J1740–3052 yield a characteristic age of  $\tau_c = P/2\dot{P} = 3.5 \times 10^5$  yr, and a relatively high implied surface dipole magnetic field strength of  $B_0 = 3.2 \times 10^{19}(P\dot{P})^{1/2} = 3.9 \times 10^{12}$  G. The pulsar is clearly young and the high magnetic field and long period suggest that it has not undergone accretion of mass and angular momentum from its companion.

Using the Taylor & Cordes (1993) model for the free electron density distribution in the Galaxy and the measured DM, we obtain an estimated distance for PSR J1740–3052 of 11 kpc, with a nominal uncertainty of about 25%.

A lower limit on the companion mass  $m_2$  can be derived from the mass function, assuming that the pulsar mass is  $m_1 = 1.35 M_\odot$ , as observed for neutron stars in binary radio pulsar systems (Thorsett & Chakrabarty 1999):

$$f_1(m_1, m_2, i) = \frac{(m_2 \sin i)^3}{(m_1 + m_2)^2} = \frac{4\pi^2}{T_\odot} \frac{x^3}{P_b^2} = \frac{4\pi^2}{T_\odot} \frac{(a_1 \sin i)^3}{c^3 P_b^2}, \quad (1)$$

where  $x = a_1 \sin i/c$  is the projected semi-major axis of the pulsar orbit,  $P_b$  is the orbital period,  $c$  is the speed of light and  $T_\odot \equiv GM_\odot/c^3 = 4.925490947 \mu\text{s}$ . Taking  $\sin i=1$ , the minimum companion mass is  $11 M_\odot$ , and the mass derived using the median inclination angle of  $i = 60^\circ$  is roughly  $16 M_\odot$ . This suggests that the pulsar companion is either a black hole or a non-degenerate star even more massive than the Be-star companion (SS2883) of PSR B1259–63. If the companion is non-degenerate, the high mass implies that it must be either an early main sequence B star or else a late-type supergiant. We will consider these two cases and that of a black hole in discussing the implications of our observations, in the end coming to the conclusion that a B star is the most likely companion, although we have no direct evidence for such a star at the pulsar’s position.

An important point to consider is the size of the companion. An early B star of  $11 M_\odot$  is expected to have a radius of 6 or  $7 R_\odot$  (e.g., Cox 2000), much smaller than the pulsar orbit. Of course, a black hole will also fit this criterion. Late-type supergiants, on the other hand, have typical radii of several hundred  $R_\odot$  (e.g., van Belle et al. 1999), comparable to or larger than the pulsar’s projected orbital semi-major axis of 757 light-seconds, which is about  $325 R_\odot$  or 1.5 AU. The distance of closest approach of the two bodies may be as small as 0.72 AU, depending on the orbital inclination angle. However, to date, there has been no evidence of eclipse of the pulsar at any phase of the orbit (§4.1). Furthermore, the youth of the pulsar and eccentricity of the orbit indicate that no significant mass has been transferred from the companion to the pulsar. Thus, if the companion is in fact a late-type supergiant, it must be confined within its Roche lobe. We use the formula of Eggleton (1983) to estimate the radius of the Roche lobe of the companion star near periastron, arriving at roughly 0.4 AU for stellar masses in the range  $11 M_\odot$  to  $16 M_\odot$ . A late-type companion must therefore have a radius smaller than this, unusually small for such a star. On the assumption that the star fills (or nearly fills) its Roche lobe, the lack of eclipses requires the inclination angle to be  $\lesssim 70^\circ$ , resulting in a companion mass of  $\gtrsim 12.5 M_\odot$ .

## 2.4 The Advance of Periastron

As mentioned in §2.3, the pulsar timing solution shows an advance of periastron,  $\dot{\omega} = 0.00021(7)^\circ \text{yr}^{-1}$ . This may be due to a combination of general-relativistic and classical

effects. For a compact companion, general relativity predicts an advance of

$$\begin{aligned}\dot{\omega} &= 3 \left( \frac{P_b}{2\pi} \right)^{-5/3} [T_\odot(m_1 + m_2)]^{2/3} (1 - e^2)^{-1} \\ &= 0.00023 \text{ } {}^\circ \text{yr}^{-1},\end{aligned}\quad (2)$$

where  $e$  is the orbital eccentricity and we assume a pulsar mass of  $m_1 = 1.35 M_\odot$  and a companion mass of  $m_2 = 16 M_\odot$ . The observed value of  $\dot{\omega}$  is comparable to this, so that a black hole companion is certainly permitted by the observations. Classical contributions to  $\dot{\omega}$  and to  $\dot{x}$ , the derivative of the projected orbital semi-major axis, may come from a quadrupole moment of a companion star, induced either by the stellar rotation or by tides raised by the neutron star (Lai, Bildsten & Kaspi 1995; Kaspi et al. 1996; Wex 1998). For a stellar quadrupole moment  $q$ , the expected classical contributions to  $\dot{\omega}$  and  $\dot{x}$  are (Wex 1998):

$$\begin{aligned}\dot{\omega} &= \frac{3\pi q}{P_b a_1^2 (1 - e^2)^2} \left( 1 - \frac{3}{2} \sin^2 \theta + \cot i \sin \theta \cos \theta \cos \Phi_0 \right) \\ &= 830 \left( \frac{q}{\text{AU}^2} \right) \sin^2 i \left( 1 - \frac{3}{2} \sin^2 \theta + \cot i \sin \theta \cos \theta \cos \Phi_0 \right) \text{ } {}^\circ \text{yr}^{-1},\end{aligned}\quad (3)$$

$$\begin{aligned}\dot{x} &= \frac{3\pi q}{P_b c a_1^2 (1 - e^2)^2} (a_1 \sin i) \cot i \sin \theta \cos \theta \sin \Phi_0 \\ &= 3.5 \times 10^{-4} \left( \frac{q}{\text{AU}^2} \right) \sin^2 i \cot i \sin \theta \cos \theta \sin \Phi_0,\end{aligned}\quad (4)$$

where  $\Phi_0$  is the precession phase, and  $\theta$  is the angle between the orbital angular momentum and the star's spin vector or the line perpendicular to the plane of the tidal bulge.

To estimate the relative importance of the spin and tidal quadrupoles,  $q_S$  and  $q_T$ , for a B main-sequence star, we follow the reasoning of Lai, Bildsten & Kaspi (1995) and take the ratio

$$\frac{q_S}{q_T} \sim \left( \frac{P_b}{P_S} \right)^2 \frac{(m_1 + m_2)}{m_1} (1 - e)^3, \quad (5)$$

where  $P_S$  is the spin period of the star, which we estimate to be  $2 \times 10^5$  sec, similar to that for the B1V companion to PSR J0045–7319 (Bell et al. 1995). From this, we derive  $q_S/q_T \sim 10^4$ ; consequently the tidal quadrupole is negligible in equations 3–4 above.

The measured non-general-relativistic contribution to  $\dot{\omega}$  is  $\lesssim 0.00012 {}^\circ \text{yr}^{-1}$ . Assuming  $i = 60^\circ$ ,  $\theta = 20^\circ$  (Bailes 1988) and  $\Phi_0 = 45^\circ$ , we find  $q_S \lesssim 2.0 \times 10^{-7} \text{ AU}^2$ . The rotationally-induced quadrupole moment,  $q_S$ , is given by (Cowling 1938):

$$q_S = \frac{2}{3} \frac{k R_2^5 \Omega^2}{G m_2} \quad (6)$$

where  $G$  is Newton's constant,  $\Omega = 2\pi/P_S$  is the stellar angular velocity,  $m_2$  and  $R_2$  are

the companion mass and radius, and  $k$  is the apsidal constant representing the structure of the star, estimated for such a star to be  $\sim 0.01$  (Schiff 1958; Claret & Gimenez 1992). With a radius estimate of  $6.5 R_\odot$  as for the companion to PSR J0045–7319 (Bell et al. 1995), this leads to an estimate of the stellar rotational angular velocity of  $\Omega \lesssim 2.7 \times 10^{-5} \text{ rad s}^{-1}$ ,  $P_S \gtrsim 2.3 \times 10^5 \text{ s}$ , consistent with that used above in equation 5.

Based on this estimate of the spin quadrupole, the change in the projected semi-major axis is predicted to be  $\dot{x} \lesssim 4.6 \times 10^{-11} \sin^2 i \cot i \sin \theta \cos \theta \sin \Phi_0$ , comparable to our measured limit of  $4 \times 10^{-11}$  and providing no constraints on the inclination angle or precession phase.

In the case of a late-type companion, we estimate  $R_2 \sim 0.35 \text{ AU}$  based on the Roche lobe argument in §2.3,  $m_2 = 12.5 M_\odot$ ,  $i = 70^\circ$  and  $k \sim 0.03$  (A. Claret, private communication). The spin of the star,  $\Omega$ , is not well known. Based on an estimate of  $v \sin i \simeq 1 \text{ km s}^{-1}$  for late supergiants (de Medeiros & Mayor 1999), we arrive at  $\Omega \simeq 1.2 \times 10^{-7} \text{ rad s}^{-1}$ , and hence  $q_S \simeq 3.0 \times 10^{-6} \text{ AU}^2$  for a  $12.5 M_\odot$  star. However, as the radius of the star must be significantly smaller than that of most supergiants,  $v \sin i$  could well be larger. An estimate of  $\Omega \simeq 3.1 \times 10^{-7} \text{ rad s}^{-1}$  and hence  $q_S \simeq 2.0 \times 10^{-5} \text{ AU}^2$  comes from setting the stellar rotational rate equal to the orbital frequency.

The quadrupole moment due to a tide,  $q_T$ , can be written as:

$$q_T = k \frac{m_1}{m_2} R_2^2 \left( \frac{R_2}{r} \right)^3 \quad (7)$$

where  $r$  is the centre-of-mass separation at any given time (Lai, Bildsten & Kaspi 1995). Under the same assumptions given above for a late-type companion, we find  $q_T \simeq 5.3 \times 10^{-6} \text{ AU}^2$  averaged over the orbit. Thus the static tidal and the rotational quadrupole moments may well be roughly the same order of magnitude, although probably not aligned.

The tidal quadrupole will not contribute to the value of  $\dot{x}$  in equation 4 above, as the tidal bulge will be aligned with the orbital plane. The measured limit of  $\dot{x} < 4.0 \times 10^{-11}$ , combined with the assumptions that  $i = 70^\circ$  and  $\theta = 20^\circ$ , yields a value of  $q_S \lesssim 1.6 \times 10^{-6} \text{ AU}^2$  or  $\Omega \lesssim 8.0 \times 10^{-8} \text{ rad s}^{-1}$  for  $\Phi_0 = 45^\circ$ , slightly smaller than our estimate above.

However, both the static tidal and rotational quadrupole moments will contribute to the value of  $\dot{\omega}$ , although, given the difference in magnitudes and alignments, the contributions will differ in size and perhaps also in sign. Using the estimate of  $q_S$  derived in the preceding paragraph, we arrive at a maximum rotational quadrupole contribution to  $\dot{\omega}$  of  $0.0013 \text{ }^\circ \text{yr}^{-1}$ . The estimate of the static tidal contribution is larger,  $\sim 0.0044 \text{ }^\circ \text{yr}^{-1}$ . The actual measured

value of  $\dot{\omega}$  is  $0.00021(7)^\circ\text{yr}^{-1}$ , about an order of magnitude smaller than either of these values.

With the simple assumptions we have made, it is difficult to reconcile the observed and predicted values of  $\dot{\omega}$  for a late-type supergiant companion. It may be possible to do so through fine-tuning of the stellar spin, the precession phase and the spin inclination angle, but such a solution seems unlikely.

### 3 NEAR-IR SEARCH FOR THE COMPANION

In order to clarify the nature of the companion, we undertook observations in other wavebands. PSR J1740–3052 lies only  $0^\circ.13$  from the Galactic plane, very close to the Galactic Centre and at a distance of roughly 11 kpc; large amounts of extinction are therefore expected at optical wavelengths. Indeed, there is no object at the pulsar position in the Digitised Sky Survey (DSS), which covers the  $V$ -band to approximately 16th magnitude. There is also no sign of an optical image on deeper Sky Survey photographs taken with the U.K. Schmidt Telescope, to limiting magnitudes of 21 in  $B$ , 20 in  $R$  and 18 in  $I$ . We therefore carried out observations at infrared wavelengths.

On 1999 May 2 (MJD 51300, binary phase 0.77), we obtained  $K$ -band ( $2.2\ \mu\text{m}$ ) spectroscopic observations using the MPE near-infrared imaging spectrograph 3D (Weitzel et al. 1996) on the 3.9-m Anglo-Australian Telescope (AAT), pointing at the position determined from the ATCA observation. This observation revealed a bright star with  $K$ -band magnitude of  $10.05 \pm 0.05$  within  $1''$  of the nominal position. The observations were made using the tip-tilt correction system ROGUE (Thatte et al. 1995). 3D uses an integral field unit to split the light from a spatial grid of  $16 \times 16$  0.4 arcsec pixels into 256 separate spectra. The effective resolution,  $\lambda/\Delta\lambda$ , of 1100 is obtained by combining two spectra whose wavelength centre is shifted by half a pixel using a piezo-driven flat mirror. We observed HD161840 (spectral type B8V) as an atmospheric standard. A Lorentzian was fitted to the hydrogen Brackett- $\gamma$  absorption during reduction. We also observed HD169101 (spectral type A0V) as a flux calibrator, assuming  $V - K = 0$ . Data were reduced using routines written for the GIPSY data reduction package (van der Hulst et al. 1992). The reduction sequence involved flat fielding, bad pixel correction, merging of the separate images corresponding to the two sub-spectra, wavelength calibration, and formation of a data cube. The final spectrum of the

source, which had an effective integration time per pixel of 1680 seconds, was then extracted from the merged cube, and divided by the atmospheric standard.

At the same time, we obtained a  $2' \times 2'$   $K$ -band image of the field using the near-infrared array camera CASPIR (McGregor et al. 1994) on the Australian National University 2.3-m telescope at Siding Spring Observatory. The exposure time was 1 minute, and the limiting  $K$  magnitude was  $\sim 17$ . This image is shown in Fig. 4.

The bright star from the 3D observation was identified on the CASPIR image as shown in Fig. 4, with a consistent  $K$ -band magnitude of  $10.03 \pm 0.01$ . Astrometric reduction of this image was performed at the Royal Observatory Edinburgh. Twelve secondary reference stars were identified on both the  $K$ -band image and an archival UK Schmidt Telescope  $R$ -band plate. Positions of these stars and hence the candidate star were related to the Hipparcos reference frame using the Tycho-AC catalogue (Urban, Corbin & Wycoff 1998) and SuperCOSMOS digitised images (Hambly et al. 1998). This yielded a position for the star of R.A.(2000)  $17^{\text{h}}40^{\text{m}}50\overset{\text{s}}{.}01(1)$ , Dec.(2000)  $-30^{\circ}52'03\overset{\text{s}}{.}8(2)$ . Within the combined errors, this position agrees with the position of the pulsar given in Table 1. A simple count yields a density of objects bright enough to be detected in the CASPIR image of roughly 0.015 per  $\text{arcsec}^2$ . Using an error region of  $0.86 \text{ arcsec}^2$ , which includes the 95% confidence regions for both the radio and optical positions, the probability of a chance coincidence is 1.3%.

We note that the candidate companion star is included in the Point Source Catalogue of the Two Micron All Sky Survey (2MASS) collaboration, with the designation 2MASSI 1740500–305204. In an observation on 1998 Aug. 14 (binary phase 0.64), the survey determined  $J$ ,  $H$  and  $K$  apparent magnitudes of  $14.523 \pm 0.046$ ,  $11.441 \pm 0.024$ , and  $10.009 \pm 0.030$ , respectively. Within the uncertainties, therefore, the star appears to be stable in magnitude.

The  $K$ -band spectrum obtained with the AAT is shown in Fig. 5, with the most prominent lines indicated. There is significant absorption of metals and both  $^{12}\text{CO}$  and  $^{13}\text{CO}$ . We have compared the spectrum with those of catalogue sources (Kleinmann & Hall 1986; Wallace & Hinkle 1997) by eye and by calculating equivalent widths. The results indicate that the star is likely to have a spectral type between K5 and M3.

Figure 5 also indicates hydrogen Brackett- $\gamma$  in emission. The presence of this line in late-type stars is usually taken to indicate the presence of a compact companion with a hot accretion disk providing the ionising flux, for example, as in the X-ray binary GX1+4 (Chakrabarty & Roche 1997; Davidsen, Malina & Bowyer 1977). In the case of PSR J1740–3052,

we believe there is no accretion disk (see §4.3 below), and so the heating photons must have another source. In principle, they could come from a shock at the interface between the pulsar and supergiant winds. However, at the nominal distance of 11 kpc, the observed strength of the Brackett- $\gamma$  is 20% of the pulsar's spin-down luminosity; as Brackett- $\gamma$  is only one of many recombination lines of ionised hydrogen, we argue that the pulsar cannot provide sufficient energy to produce the observed line strength.

Because of this dilemma, further  $K$ -band spectroscopic observations of the late-type star were made using CASPIR on the 2.3-m telescope at Siding Spring Observatory on 2000 Nov. 4 (binary phase 0.16). The A0 star BS6575 was used as flux calibrator, with interpolation over Brackett- $\gamma$  during reduction. This observation gave a spectrum similar in appearance to that in Fig. 5 but with no significant indication of Brackett- $\gamma$ . As a further check, a K5 star (BS6842) and an M1 star (BS6587) were used as calibration for the supergiant spectrum – in no case was significant Brackett- $\gamma$  seen. It therefore appears that the Brackett- $\gamma$  emission seen in Fig. 5 is highly variable. Variable Brackett- $\gamma$  emission is seen in late-type stars which vary in magnitude (Lançon & Wood 2000) but it is difficult to explain in an apparently stable star such as this one. Perhaps the star is indeed variable, and the three different observations happen to have been taken at the same pulsational phase. We note that the spacing in days between the two CASPIR observations is roughly twice that between the 2MASS observation and the initial CASPIR/3D observation.

The 2MASS observations can be used to determine the extinction toward the star and hence its bolometric magnitude. For spectral types ranging from K5 to M3, the intrinsic  $J - K$  colour should be between 0.99 and 1.12, and the intrinsic  $H - K$  colour between 0.19 and 0.25 (Houdashelt et al. 2000). Using the standard universal extinction law (Rieke & Lebofsky 1985) to derive  $A_K/E(J - K) = 0.66$  and  $A_K/E(H - K) = 1.78$ , we find that the  $K$ -band extinction  $A_K$  must be in the range 2.1 to 2.3 magnitudes. The  $K$ -band bolometric correction is approximately 2.6 for a K5 star and 2.7 for an M3 star (Houdashelt et al. 2000). Thus if the star were at the estimated pulsar distance of  $\sim 11$  kpc, the observed  $K$  magnitude of about 10.03 would imply a bolometric magnitude in the range  $-4.6$  to  $-4.9$ . This luminosity implies a stellar mass of only  $6$  to  $7 M_\odot$  for a supergiant (Maeder & Meynet 1989), not large enough to make this star the pulsar companion.

It is well recognised that distances estimated from the Taylor & Cordes (1993) dispersion measure model may be significantly in error. The models of Maeder & Meynet (1989) predict a bolometric magnitude of  $-6.5$  for a  $12 M_\odot$  star, requiring the system to be at a distance

of 23 kpc — more than twice as far as predicted by the dispersion measure model. We do not believe this to be likely, but it is not impossible.

A further problem which arises with identifying this star as the companion, at either distance, is the stellar radius. As noted in §2.3, red supergiants have radii of several hundred  $R_{\odot}$  (van Belle et al. 1999), larger than permitted by the pulsar orbit. In fact, requiring that the companion be contained within the Roche lobe forces the stellar radius to be less than 0.4 AU. In short, the luminosity and radius required of a late-type supergiant make it quite unlikely that this star is the pulsar companion. If the observed star lies near the Galactic centre at a distance of 8.5 kpc, its bolometric luminosity would be approximately  $-4.3$ , consistent with that of the roughly solar-mass red giants which dominate the Galactic Bulge stellar population. We believe that this is the most self-consistent explanation of the properties of this star.

It therefore appears that the positional agreement between the late-type star and the pulsar is indeed a coincidence. If there were to be a B star hidden by the light of the late-type star and at the estimated pulsar distance of 11 kpc, its  $K$ -band magnitude would be roughly 15 and it would not appreciably change the observed  $K$ -band spectrum.

## 4 OBSERVATIONS NEAR PERIASTRON

In a further attempt to distinguish between a black hole and a non-degenerate companion, we undertook dual-frequency radio monitoring campaigns of the pulsar around the periastrons of 2000 February 10 (MJD 51584.5) and 2000 September 28 (MJD 51815.5). Observations were made at Parkes on most days in the periods 2000 February 5 – 17 and 2000 September 19 – 30 at centre frequencies of 660 MHz and 1390 MHz. The goals of these campaigns were to verify the absence of eclipses and to look for evidence of variations in the pulsar’s dispersion and rotation measures, as such changes might be expected from the interaction of the pulsar signal with the wind from a non-degenerate companion.

### 4.1 Timing Observations

The Parkes dual-frequency timing observations were performed at 660 MHz using a  $2 \times 256 \times 0.125$ -MHz filterbank and, using the central beam of the multibeam receiver, at 1390 MHz with a  $2 \times 512 \times 0.5$ -MHz filterbank, both employing the 1-bit digitisation system described in §2.1. The pulsar was detected on each observing day, demonstrating conclusively that

there is no eclipse. Fig. 6 shows timing residuals of the 660-MHz and 1390-MHz data as a function of orbital phase, with the dispersion measure held constant at the value given in Table 1. There is clear evidence for increased and variable dispersion before periastron. This pattern is consistent with the observed longitude of periastron, as the companion is between us and the pulsar before periastron and beyond the pulsar after periastron. Therefore, one would expect increased DMs before periastron and more stable values after.

These observations show that the increase in DM on any given day relative to the reference DM of  $740.9(2) \text{ cm}^{-3} \text{ pc}$  is typically of the order of 1 or  $2 \text{ cm}^{-3} \text{ pc}$ . For the observations before periastron, the extra distance travelled across the pulsar orbit is about  $10^{13} \text{ cm}$ , or 0.67 AU, leading to an estimated electron density inside the orbit of a few  $\times 10^5 \text{ cm}^{-3}$ .

We consider once again the possibility of a late-type, cool, bright star as the companion. The expected stellar wind from such a star is of the order of  $10^{-6} M_\odot \text{ yr}^{-1}$  (e.g., Dupree 1986) with an ionised fraction of 0.002 – 0.02 (Drake & Linsky 1983). The closest approach of the two stars for  $i = 70^\circ$ ,  $m_2 = 12.5 M_\odot$  is only 0.75 AU, just twice the maximum possible stellar radius based on Roche-lobe considerations. Assuming a distance from the companion centre of about 0.75 AU and a stellar wind velocity of  $\sim 30 \text{ km s}^{-1}$  (Dupree 1986), we arrive at an estimate for an ionised mass-loss rate of a few  $\times 10^{-11} M_\odot \text{ yr}^{-1}$  and therefore an overall mass-loss rate of  $10^{-9}\text{--}10^{-8} M_\odot \text{ yr}^{-1}$ . This is smaller by two orders of magnitude than the expected rate for these stars, which could possibly be explained if the mass loss is very clumpy as found, for example, in  $\alpha$  Ori (e.g., Skinner & Whitmore 1987). However, we believe that this low mass-loss rate casts further doubt on the association of the late-type star with the pulsar.

In the case of an early B star, we follow the arguments of Kaspi et al. (1996) and references therein in adopting the following law for the wind velocity  $v_w$ :

$$v_w(r) = v_\infty (1 - R_2/r)^{1/2}, \quad (8)$$

where  $r$  is the distance from the centre of mass of the star and  $v_\infty$  is 1–3 times the escape velocity  $v_{\text{esc}} \approx 725 \text{ km s}^{-1}$ . The electron density  $n_e(r)$  at any point  $r$  from the star can be found from mass conservation:

$$\dot{M} = 4\pi r^2 n_e(r) m_p v_w(r) \quad (9)$$

where  $\dot{M}$  is the mass-loss rate and  $m_p$  is the proton mass. For the observations just before periastron, we integrate numerically along the line of sight through the pulsar orbit in the following manner:

$$I = \int \frac{1}{\sqrt{1 - R_2/r}} \frac{1}{r^2} dl \quad (10)$$

in order to find the expected difference in DM. The end result is:

$$\dot{M} = 1.1 \times 10^{-9} \left( \frac{v_\infty}{v_{\text{esc}}} \right) \frac{\Delta \text{DM}}{I} M_\odot \text{yr}^{-1} \quad (11)$$

where  $\Delta \text{DM}$  is the difference in DM before and after periastron in units of  $\text{cm}^{-3} \text{pc}$  and  $I$  is in units of  $\text{AU}^{-1}$ . Both  $\Delta \text{DM}$  and  $I$  are of the order of unity here, implying a mass-loss rate of a few  $\times 10^{-9} M_\odot \text{yr}^{-1}$ , roughly what is predicted for early-type stars of this mass in the Galaxy (e.g., de Jager et al. 1988). We note that this mass-loss rate is two orders of magnitude higher than the upper limit found for PSR J0045–7319 in the Small Magellanic Cloud, lending support to the argument for a metallicity dependence of the mass-loss rate for such stars (Kaspi, Tauris & Manchester 1996).

We conclude that the observed DM variations are better explained by an early B-star companion rather than by a late-type supergiant.

## 4.2 Polarimetric Observations

The polarisation of the mean pulse profile was measured on a total of 18 days before, during and after the 2000 February periastron, and on several other occasions throughout the orbit, using the centre beam of the multibeam receiver and the Caltech correlator (Navarro 1994). The centre frequency and bandwidth were 1318.5 MHz and 128 MHz, respectively. Observations were made in pairs at orthogonal position angles, typically for 30 min at each angle; summing of these orthogonal pairs removes most of the effects of instrumental polarisation. Data were calibrated following standard procedures (Navarro et al. 1997), except that the full frequency resolution of the correlator,  $128 \times 1 \text{ MHz}$ , was retained during the processing.

In general, the mean pulse profile is weakly polarised. Fig. 7 shows the mean profile resulting from adding all of the data obtained over the periastron period, between 2000 February 4 and February 17, a total of 5.85 hours of observation. The average linear polarisation  $\langle L \rangle / \langle I \rangle$ , where  $L = (Q^2 + U^2)^{1/2}$ , is only  $1 \pm 4\%$ . However, there is some significant circular polarisation, with a hint of a sense reversal near the pulse peak. This suggests that the very narrow pulse (full width at half-maximum of  $8^\circ$  of longitude) is from the core region of the polar cap (e.g., Rankin 1983).

It is possible that the very low linear polarisation is due to Faraday depolarisation in the wind of the companion. This effect is seen in the eclipsing Be-star system PSR B1259–63

(Johnston et al. 1996). To investigate this we summed the individual channel data for each orthogonal pair over a range of rotation measures (RM) from  $-5000$  to  $+5000$  rad m $^{-2}$  in steps of 50 rad m $^{-2}$ . Where significant linear polarisation was found, an improved value of the rotation measure was computed from a weighted mean position angle difference between the two halves of the observed band. On three of 20 or so observations made away from periastron, on 2000 February 28, March 26 and May 31, significant linear polarisation (20–30%) was observed with rotation measures of +180, −85, and −220 rad m $^{-2}$ , respectively. No significant polarisation (< 10%) was observed at any rotation measure within the search range during the periastron period or on other occasions.

These results suggest that Faraday rotation is occurring in the wind of the companion star and that it is highly variable. Combined with the DM variations of 1 or 2 cm $^{-3}$  pc during periastron passage (§4.1), the RM changes indicate that the magnetic field strength in the wind region (weighted by the local electron density) is at least a few times 0.1 mG. The observed variations suggest that the field structure is complex, and so this value, which is integrated along the line of sight, is a lower limit to the actual field strength in the wind region.

The very existence of DM and RM variations appears to argue against a black hole as the pulsar companion, although it is perhaps plausible that the passage of the signal through the extended atmosphere of the late-type star could be responsible for the variations if the late-type star is foreground and the geometry is favourable.

### 4.3 Archival X-ray Observations

For a non-degenerate companion, particularly an extended giant star, accretion of companion wind material onto the neutron star could in principle occur near periastron, where the distance of closest approach is  $0.72 \text{ AU}/\sin i$ . Such accretion might result in observable X-ray emission.

To investigate this possibility, we examined archival X-ray observations of the field near PSR J1740–3052. Serendipitously, the *ASCA* X-ray telescope (Tanaka, Inoue & Holt 1994) observed a field containing PSR J1740–3052 on 1995 September 26 (Sequence ID 53016050) as part of its survey of Galactic Ridge emission. This is only 19 days after a periastron passage. In addition, the source was only 8' from the centre of the field of view in the observation.

We have reduced data from the two co-aligned Gas Imaging Spectrometers (GIS) onboard *ASCA*. The effective total GIS exposure was  $2 \times 12.5$  ks. We used the standard *ASCA* data analysis tool `XSELECT` to produce a first image of the field, for both GIS2 and GIS3. For this image, we included counts having energies between 2 and 10 keV, as softer emission is likely to have been absorbed, given the large expected column density toward the source (see below). The resulting image was exposure-corrected, and was further corrected for variations in the particle background over the fields-of-view using the `FTOOL ascaexpo`. For details, see Roberts, Romani & Kawai (2001). The corrected GIS2 and GIS3 images were combined and smoothed with a Gaussian function having FWHM 50''.

No significant emission was detected from the pulsar position. To set an upper limit on the flux, we first found the rms scatter of the image,  $1.5 \times 10^{-7}$  counts  $\text{s}^{-1} \text{cm}^{-2} \text{pixel}^{-1}$ . This number was then multiplied by the number of pixels (117) in the half-power region of the *ASCA* point-spread function. Multiplying by 2 for the full power, and by 3 to yield a  $3\sigma$  upper limit, we find that the observed flux from the source in the 2–10 keV band is  $< 1 \times 10^{-4}$  counts  $\text{s}^{-1} \text{cm}^{-2}$ .

In order to determine the upper limit on the energy flux and hence source luminosity, we assume a simple power-law model having photon index  $-2$ , and an equivalent neutral-hydrogen absorbing column of  $N_H \simeq 3 \times 10^{22} \text{ cm}^{-2}$ . We use HEASARC's tools<sup>¶</sup> to convert the above upper limit on the photon flux into an upper limit on the unabsorbed energy flux,  $1.4 \times 10^{-12} \text{ erg s}^{-1} \text{ cm}^{-2}$ , in the 2–10 keV band. For a distance of 11 kpc as estimated from the pulsar's dispersion measure (see §2.3), this implies an upper limit on the source's 2–10 keV luminosity  $L_x < 2 \times 10^{34} \text{ erg s}^{-1}$ . Assuming the simplest possible accretion model, this implies  $\dot{M} < L_x R_p / G m_1 = 1.8 \times 10^{-12} M_\odot \text{ yr}^{-1}$ , where  $R_p = 10 \text{ km}$  and  $m_1 = 1.35 M_\odot$  are the assumed neutron star radius and mass, respectively.

Given this upper limit, accretion is very unlikely to have occurred. Such a low  $\dot{M}$  is unlikely to have sufficient pressure to overcome the pulsar wind pressure (see, e.g., Tavani, Arons & Kaspi 1994), so material is unlikely to have come within the accretion radius. We note however that our upper limit does not preclude the existence of non-thermal shock-powered X-rays like those seen in the pulsar/Be star binary PSR B1259–63 near periastron (Kaspi et al. 1995; Hirayama et al. 1996). The shock emission is ultimately powered by the pulsar's spin down. PSR J1740–3052 has a much smaller spin-down luminosity than

<sup>¶</sup> `WebSpec`: <http://heasarc.gsfc.nasa.gov/cgi-bin/webspec> and `W3PIMMS`: <http://heasarc.gsfc.nasa.gov/Tools/w3pimms.html>.

PSR B1259–63 and is much more distant. Even in the unlikely event that *all* of the spin-down luminosity of PSR J1740–3052 ( $\dot{E} = 5.5 \times 10^{33}$  erg s $^{-1}$ , see Table 1) were converted into shock emission in the X-ray band, it would be unobservable in the archival *ASCA* data.

## 5 DISCUSSION

On evolutionary grounds, there is no reason to prefer one type of candidate companion over another. As we have discussed above, PSR J1740–3052 is a young pulsar which has not undergone an episode of mass transfer from its companion. The pulsar’s characteristic age is  $3.5 \times 10^5$  yr, while a late-type supergiant star might be expected to evolve from an OB star in  $\sim 10^7$  yr, making either type of non-degenerate companion consistent from the point of view of stellar ages. The fact that the system remained bound on formation of the neutron star suggests that the pre-supernova star was the less massive of the two at the time of the explosion. This is consistent with evolutionary scenarios involving mass transfer on to the initially lighter star (Portegies Zwart & Yungelson 1998). This mass transfer may also have somewhat accelerated the companion’s evolution. Alternatively, a suitably oriented kick on formation could have kept the system bound (Bailes 1988; Tauris & Takens 1998). In the case of a black-hole companion, the neutron star would be the second-formed compact object, as the black-hole progenitor would have been more massive initially.

Two pulsar systems are currently known to have non-degenerate companion stars, PSRs B1259–63 (Johnston et al. 1992) and J0045–7319 (Kaspi et al. 1994), and these contain Be and B stars, respectively. These systems are considered likely progenitors of HMXBs. If, as we believe is likely, the companion to PSR J1740–3052 is also an early B star, then this system will likely also become an HMXB in the future, as the neutron star begins to accrete matter from the evolving companion’s wind. As the companion evolves to overflow its Roche lobe, the system will enter a common-envelope phase and the neutron star will begin to spiral in. The current orbital period of this system, 231 days, makes the outcome after this point uncertain (van den Heuvel 1993). The neutron star may spiral in completely, resulting in a red giant star with a neutron star core: a Thorne-Zytkow object (Thorne & Zytkow 1977). Alternatively, there may be enough energy released during the orbital spiral-in to eject the common envelope, leaving behind the evolved core of the companion. Given the current mass of the companion, this core is likely to undergo a supernova explosion itself, leaving behind either

a bound double-neutron-star system such as PSR B1913+16, or else two isolated neutron stars, one mildly recycled, one young.

We have argued throughout this paper that the companion is most likely to be an early-type B star rather than a black hole or the late-type star which is coincident with the pulsar's position. Our arguments may be summarized as follows:

- (i) The magnitude of the late-type star coincident with the pulsar position can be made consistent with the bolometric magnitude of an  $11 M_{\odot}$  star only if the dispersion measure estimate of the distance to the pulsar is low by a factor of two. In contrast, the colours and magnitude of the star are perfectly consistent with an AGB star of about  $1 M_{\odot}$  at the Galactic centre.
- (ii) An early-B main sequence star at the nominal pulsar distance of about 11 kpc and hidden by the late-type star would not significantly alter the observed  $K$ -band magnitude or spectrum.
- (iii) The radii of late-type supergiant stars are as large as or larger than the pulsar's orbit. No significant mass has been transferred to the pulsar from the companion, requiring the companion to be confined inside its Roche lobe of radius roughly 0.4 AU, improbably small for a late-type supergiant. Such a small radius would also require either a higher temperature or a smaller luminosity for the star, contrary to our understanding of the evolution of these objects (Maeder & Meynet 1989).
- (iv) Even for a late-type supergiant of the small required radius, the calculated magnitudes of the tidal and spin quadrupoles predict an advance of periastron in the pulsar's orbit an order of magnitude larger than that observed. By contrast, similar estimates for an early B star predict values not much larger than the general-relativistic prediction, and a good match to the observations. A black-hole companion is also consistent with these observations.
- (v) The existence of orbital-phase-dependent DM and RM variations argues for a non-degenerate companion of some kind, and against a black-hole companion unless there is a fortuitous alignment between the pulsar's orbit and the extended wind of the foreground late-type star. Furthermore, the observed magnitude of the DM variations implies a stellar wind two orders of magnitude smaller than that predicted for late-type stars (e.g., Dupree 1986) but consistent with that expected for an early B star.

All points considered, we find that the bulk of the evidence points to a non-degenerate

companion, but to an early B star rather than to the late-type star observed to be coincident with the pulsar position. It should be possible to establish whether or not the late-type star is the companion through a careful search for Doppler radial velocity variations in the stellar spectrum. The expected total range of radial velocity variation is  $22 \text{ km s}^{-1}$  for an  $11 M_{\odot}$  companion, or  $15 \text{ km s}^{-1}$  for a  $16 M_{\odot}$  companion; this should be measurable with a high-resolution spectrometer. Further multifrequency radio monitoring of the orbital DM and RM variations will lead to a characterization of the wind of a non-degenerate companion. Finally, continued long-term timing of the pulsar will lead to precise values of  $\dot{\omega}$  and  $\dot{x}$ , allowing a separation of general-relativistic effects from those caused by the quadrupole of a non-degenerate companion, thus providing final proof of the nature of the companion.

## ACKNOWLEDGEMENTS

We thank Steve Eikenberry, Anita Richards and Lars Bildsten for helpful discussions, Mallory Roberts for help with the X-ray reduction, and George Hobbs for help with observing. The Parkes radio telescope is part of the Australia Telescope which is funded by the Commonwealth of Australia for operation as a National Facility managed by CSIRO. IHS received support from NSERC and Jansky postdoctoral fellowships. VMK is an Alfred P. Sloan Research Fellow, and received support from an NSF CAREER award (AST-9875897), NASA grant NAG5-9120 and an NSERC grant (RGPIN228738-00). F. Camilo is supported by NASA grant NAG5-9095. This research has made use of the Astronomical Data Center (ADC) at NASA Goddard Space Flight Center, and the Simbad and Vizier services operated by CDS Strasbourg. It has also used data products from the Two Micron All Sky Survey, which is a joint project of the University of Massachusetts and the Infrared Processing and Analysis Center/California Institute of Technology, funded by the National Aeronautics and Space Administration and the National Science Foundation. The Digitised Sky Surveys were produced at the Space Telescope Science Institute under U.S. Government grant NAG W-2166.

## REFERENCES

- Bailes M., 1988, A&A, 202, 109
- Bell J. F., Bessell M. S., Stappers B. W., Bailes M., Kaspi V. M., 1995, ApJ, 447, L117
- Bhattacharya D., van den Heuvel E. P. J., 1991, Phys. Rep., 203, 1
- Chakrabarty D., Roche P., 1997, ApJ, 489, 254

Claret A., Gimenez A., 1992, *A&AS*, 96, 255

Cowling T. G., 1938, *MNRAS*, 98, 734

Cox A. N., ed, 2000, *Allen's astrophysical quantities*, 4th ed. AIP Press; Springer, New York

Davidson A., Malina R., Bowyer S., 1977, *ApJ*, 211, 866

de Jager C., Nieuwenhuijzen H., van der Hucht K. A., 1988, *A&AS*, 72, 259

de Medeiros J. R., Mayor M., 1999, *A&AS*, 139, 433

Drake S. A., Linsky J. L., 1983, *ApJ*, 274, L77

Dupree A. K., 1986, *Ann. Rev. Astr. Ap.*, 24, 377

Eggleton P. P., 1983, *ApJ*, 268, 368

Hambly N. C., Miller L., MacGillivray H. T., Herd J. T., Cormack W., 1998, *MNRAS*, 298, 897

Hirayama M., Nagase F., Tavani M., Kaspi V. M., Kawia N., Arons J., 1996, *PASJ*, 48, 833

Houdashelt M. L., Bell R. A., Sweigart A. V., Wing R. F., 2000, *AJ*, 119, 1424

Hulse R. A., Taylor J. H., 1975, *ApJ*, 195, L51

Johnston S., Manchester R. N., Lyne A. G., Bailes M., Kaspi V. M., Qiao G., D'Amico N., 1992, *ApJ*, 387, L37

Johnston S., Manchester R. N., Lyne A. G., D'Amico N., Bailes M., Gaensler B. M., Nicastro L., 1996, *MNRAS*, 279, 1026

Kaspi V. M., Johnston S., Bell J. F., Manchester R. N., Bailes M., Bessell M., Lyne A. G., D'Amico N., 1994, *ApJ*, 423, L43

Kaspi V. M., Tavani M., Nagase F., Hirayama M., Hoshino M., Aoki T., Kawai N., Arons J., 1995, *ApJ*, 453, 424

Kaspi V. M., Bailes M., Manchester R. N., Stappers B. W., Bell J. F., 1996, *Nature*, 381, 584

Kaspi V. M., Tauris T., Manchester R. N., 1996, *ApJ*, 459, 717

Kleinmann S. G., Hall D. N. B., 1986, *ApJS*, 62, 501

Lai D., Bildsten L., Kaspi V. M., 1995, *ApJ*, 452, 819

Lançon A., Wood P. R., 2000, *A&AS*, 146, 217

Maeder A., Meynet G., 1989, *A&A*, 210, 155

Manchester R. N. et al., 2001, *MNRAS*, Submitted.

McGregor P., Hart J., Downing M., Hoadley D., Bloxham G., 1994, *Experimental Astronomy*, 3, 139

Navarro J., 1994, PhD thesis, California Institute of Technology

Navarro J., Manchester R. N., Sandhu J. S., Kulkarni S. R., Bailes M., 1997, *ApJ*, 486, 1019

Phinney E. S., Kulkarni S. R., 1994, *Ann. Rev. Astr. Ap.*, 32, 591

Portegies Zwart S. F., Yungelson L. R., 1998, *A&A*, 332, 173

Rankin J. M., 1983, *ApJ*, 274, 333

Rieke G. H., Lebofsky M. J., 1985, *ApJ*, 288, 618

Roberts M. S. E., Romani R. W., Kawai N., 2001, *ApJS*, in press

Schiff L. I., 1958, *Phys. Rev. Lett.*, 1, 254

Skinner C. J., Whitmore B., 1987, *MNRAS*, 224, 335

Standish E. M., 1982, *A&A*, 114, 297

Tanaka Y., Inoue H., Holt S. S., 1994, *PASJ*, 46, L37

Tauris T. M., Takens T. M., 1998, *A&A*, 330, 1047

Tavani M., Arons J., Kaspi V. M., 1994, *ApJ*, 433, L37

Taylor J. H., Cordes J. M., 1993, *ApJ*, 411, 674

Thatte N. A., Kroker H., Weitzel L., Tacconi-Garman L. E., Tecza M., Krabbe A., Genzel R., 1995, in Fowler A., ed, *Proceedings of the SPIE*. p. 228

Thorne K. S., Źytkow A. N., 1977, *ApJ*, 212, 832

Thorsett S. E., Chakrabarty D., 1999, *ApJ*, 512, 288

Urban S. E., Corbin T. E., Wycoff G., 1998, *AJ*, 115, 2161

van Belle G. T. et al., 1999, *AJ*, 117, 521

van den Heuvel E. P. J., 1993, in Phillips J. A., Thorsett S. E., Kulkarni S. R., eds, Planets Around Pulsars. Astronomical Society of the Pacific Conference Series, p. 123

van der Hulst J. M., Terlouw J. P., Begeman K. G., Zwitser W., Roelfsema P. R., 1992, in Worrall D. M., Biemesderfer C., Barnes J., eds, ASP Conf. Ser. 25: Astronomical Data Analysis Software and Systems I. p. 131

Wallace L., Hinkle K., 1997, ApJS, 111, 445

Weitzel L., Krabbe A., Kroker H., Thatte N., Tacconi-Garman L. E., Cameron M., Genzel R., 1996, A&AS, 119, 531

Wex N., 1998, MNRAS, 298, 997

**Table 1.** Parameters of PSR J1740–3052

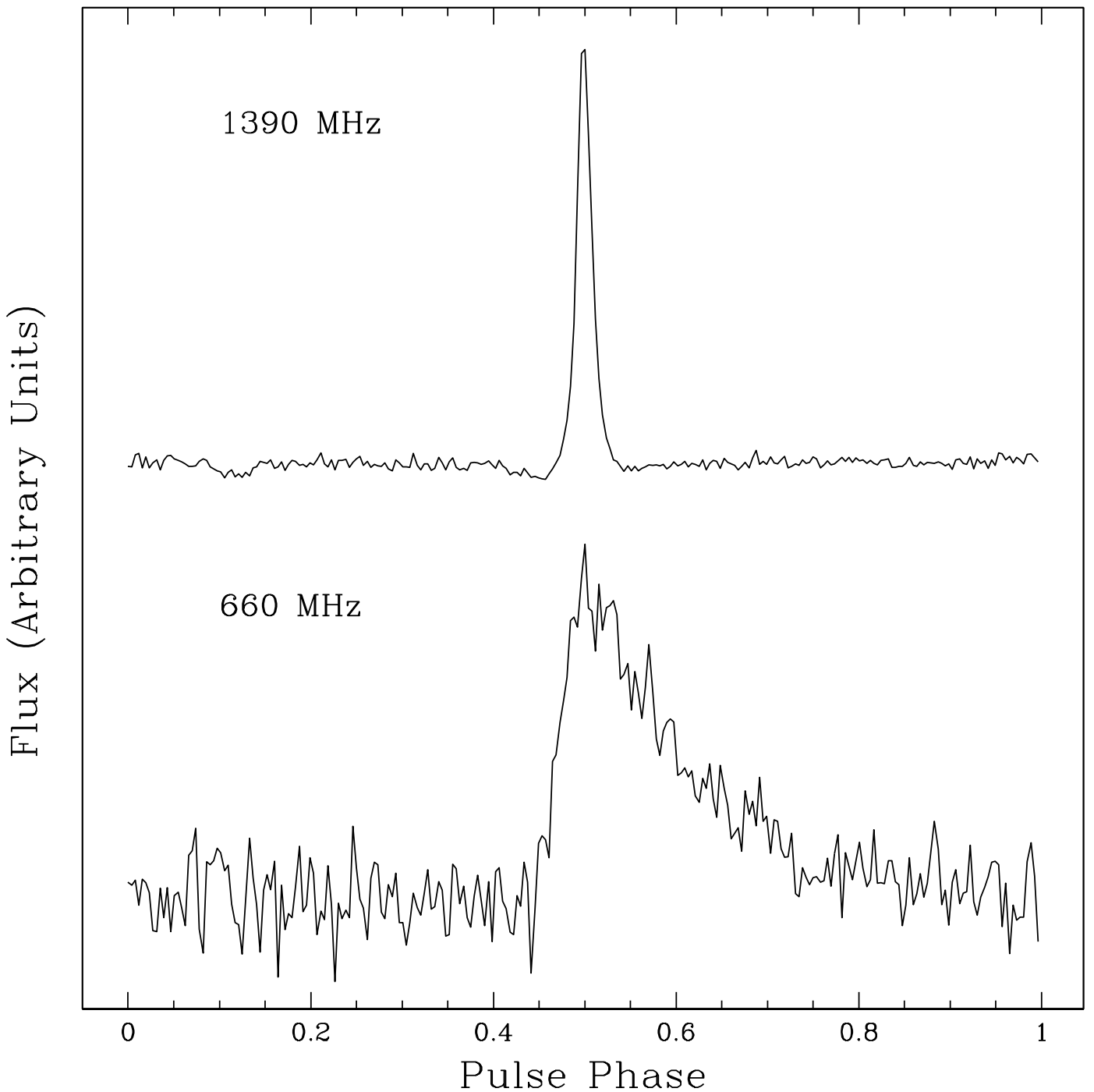
Measured Parameters	
Right Ascension (J2000) <sup>a</sup>	17 <sup>h</sup> 40 <sup>m</sup> 50 <sup>s</sup> 031(5)
Declination (J2000) <sup>a</sup>	−30°52'04.1(3)
Dispersion Measure (cm <sup>−3</sup> pc)	740.9(2)
Period (s)	0.570309580513(16)
Period Derivative	2.54969(4) × 10 <sup>−14</sup>
Epoch of Period (MJD)	51452.0
Orbital Period (days)	231.02965(3)
Projected Semi-major Axis (light-seconds)	756.9087(4)
Eccentricity	0.5788720(4)
Epoch of Periastron (MJD)	51353.51233(3)
Longitude of Periastron (degrees)	178.64613(6)
Advance of Periastron (degrees yr <sup>−1</sup> )	0.00021(7)
Derivative of Projected Semi-major Axis <sup>b</sup>	< 4 × 10 <sup>−11</sup>
Derivative of Orbital Period <sup>b</sup>	< 4 × 10 <sup>−8</sup>
Data Span (MJD)	51032 – 51872
R.M.S. Timing Residual (ms)	0.8
Flux Density at 1400 MHz (mJy)	0.7(2)

Derived Parameters	
Galactic Longitude (degrees)	357.8
Galactic Latitude (degrees)	−0.13
Distance (kpc)	~ 11
Characteristic Age (yr)	3.5 × 10 <sup>5</sup>
Surface Magnetic Field (G)	3.9 × 10 <sup>12</sup>
Rate of Energy Loss (erg s <sup>−1</sup> )	5.5 × 10 <sup>33</sup>
Mass Function (M <sub>⊙</sub> )	8.723248(12)

<sup>a</sup>Position determined from interferometric observation.

<sup>b</sup>Fit while holding all other parameters constant at the values shown.



**Figure 1.** Mean pulse profiles at 1390 MHz and 660 MHz. Integration times were 11.2 hours at 1390 MHz, and 11.6 hours at 660 MHz. The dispersion smearing is 1.11 ms at 1390 MHz, and 5.36 ms at 660 MHz. The small dip at the leading edge of the 1390-MHz profile is an instrumental artefact. The scattering timescale derived from the 660-MHz profile is roughly 58 ms. This scales by  $\nu^{-4.4}$  to about 9 ms at 1 GHz, only 25% of the value predicted by the Taylor & Cordes (1993) model.

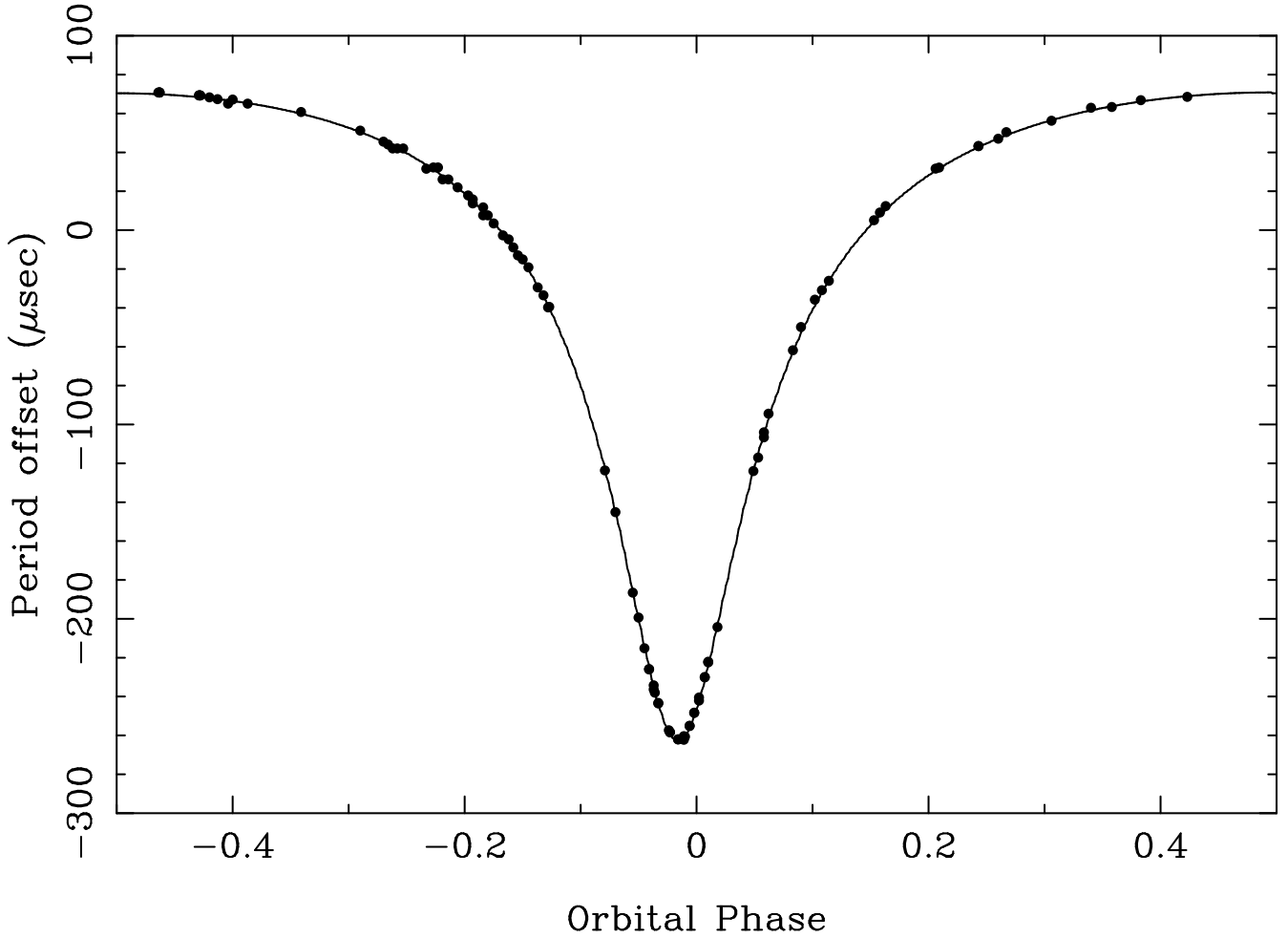


**Figure 2.** Observed variations of the solar-system barycentric period of PSR J1740–3052 over the 231-day orbital period measured using the 76-m Lovell telescope at Jodrell Bank Observatory and the 64-m telescope at Parkes. The curved line represents the fit of a binary model to the data. Orbital phase 0 is periastron, which occurs nearly in the plane of the sky.

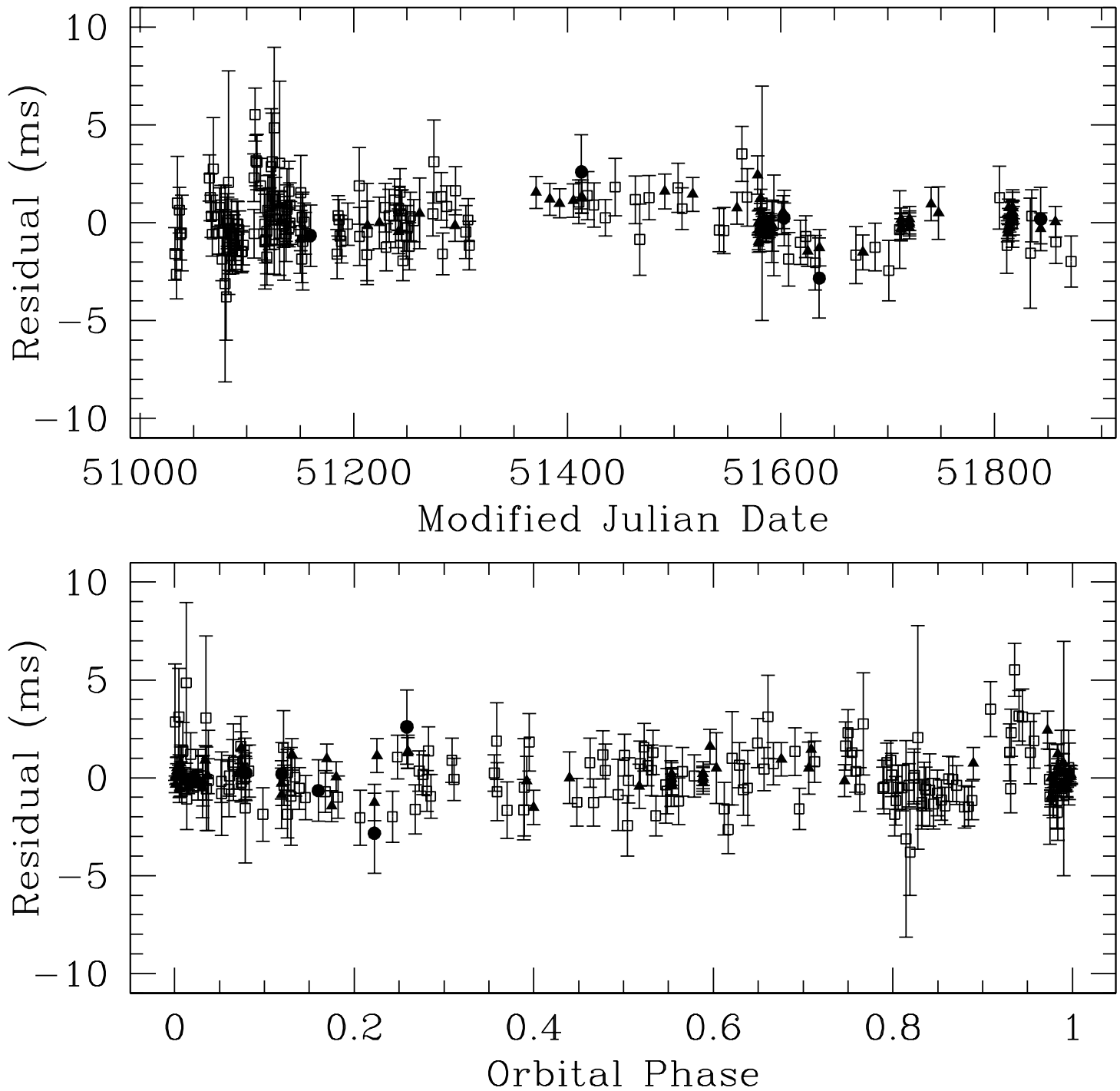


**Figure 3.** Timing residuals relative to the best-fit solution for PSR J1740–3052 over the period 1998 Aug. 7 – 2000 Nov. 23. Open squares represent Jodrell Bank 1400-MHz data, filled triangles Parkes 1400-MHz data and filled circles 660-MHz data. Top panel: residuals as a function of time. Bottom panel: residuals as a function of orbital phase, where phase 0/1 is periastron.

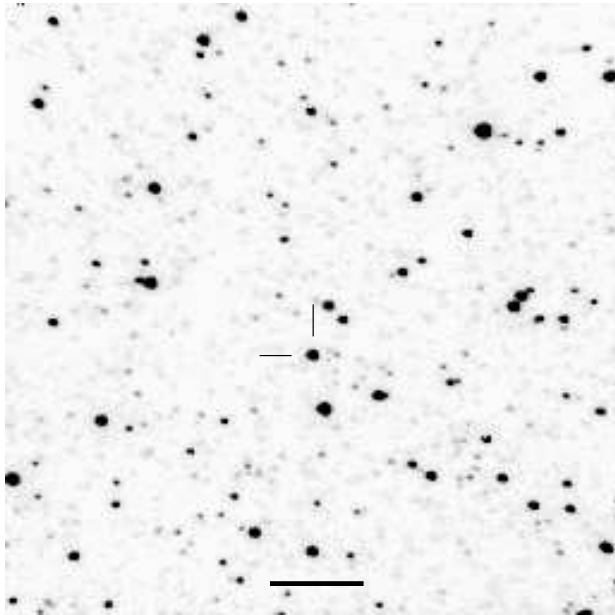


**Figure 4.** Image of the PSR J1740–3052 field taken with the Siding Spring Observatory 2.3-m telescope at  $2.2\mu\text{m}$  (K-band). The coincident late-type star, near the centre of the figure, is marked, and the thick horizontal bar is of length  $20''$ . North is at the top of the figure and east to the left.

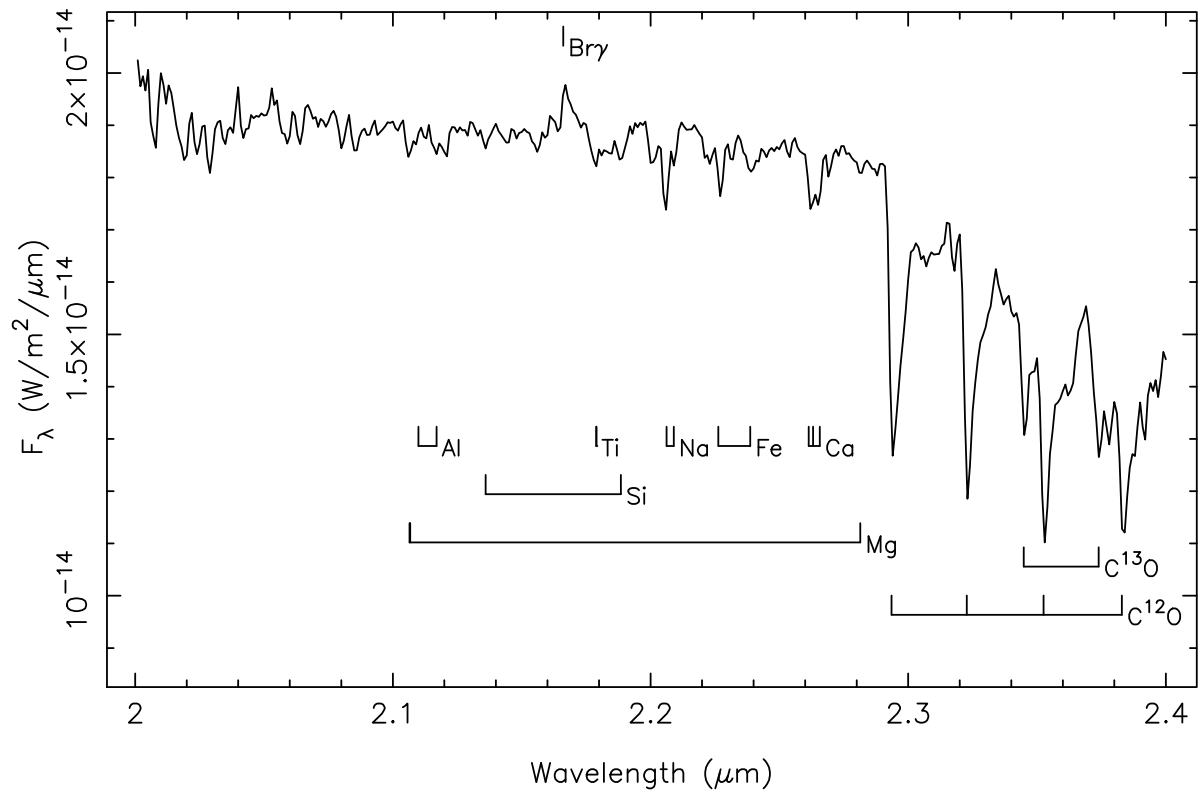


**Figure 5.**  $2.2\text{ }\mu\text{m}$  ( $K$ -band) spectrum of the late-type star at the position of PSR J1740–3052 obtained with the 3D instrument on the Anglo-Australian Telescope. Prominent spectral lines are labeled.

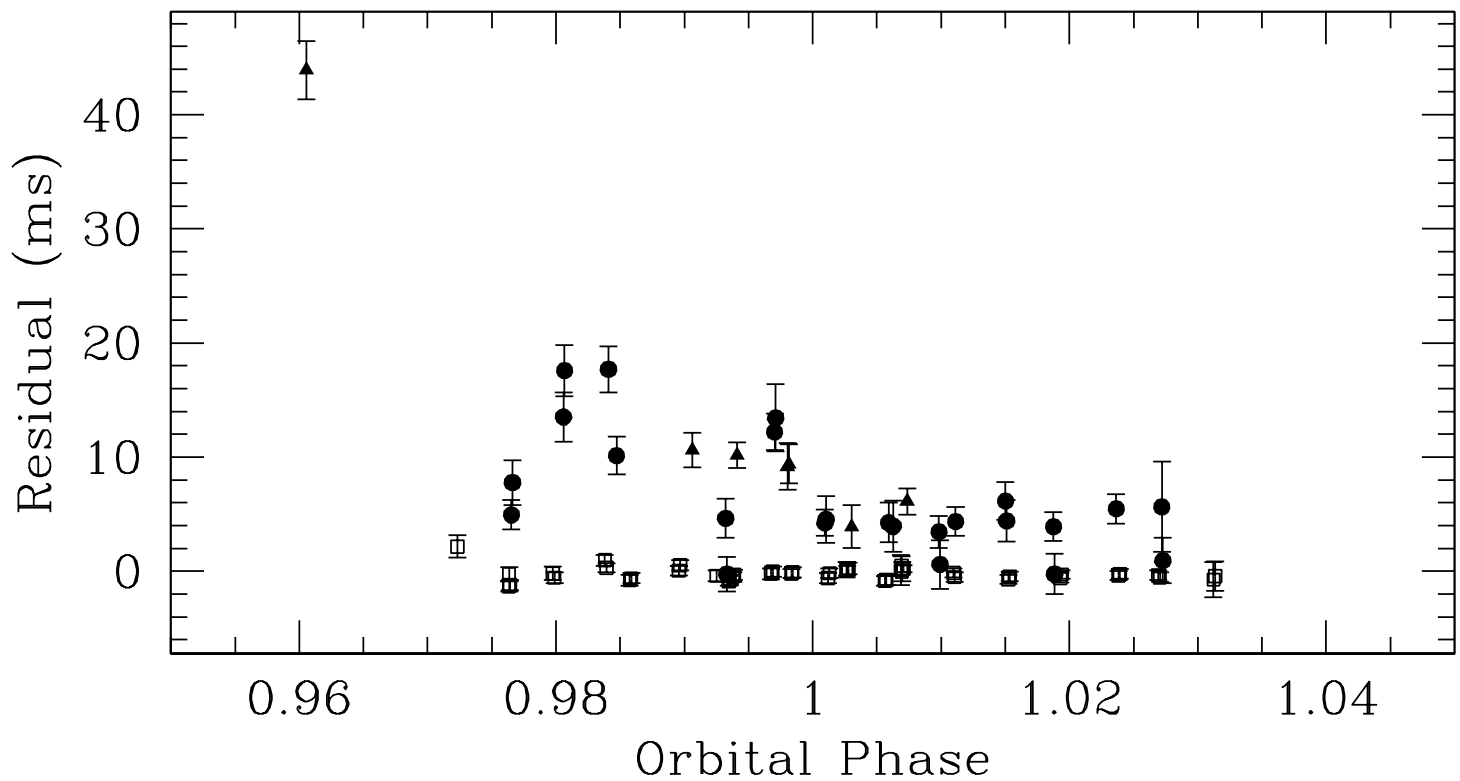


**Figure 6.** Residuals at 660 MHz and 1390 MHz as a function of orbital phase near the periastrons of 2000 February 10 and 2000 September 28. Periastron is at orbital phase 1.0. 1390-MHz data are indicated by open squares, 2000 February 660-MHz by filled circles, and 2000 September 660-MHz by filled triangles. There is clear evidence for variation in the dispersion measure before periastron. We believe the 660-MHz point at phase  $\sim 0.96$  is likely to be reliable.

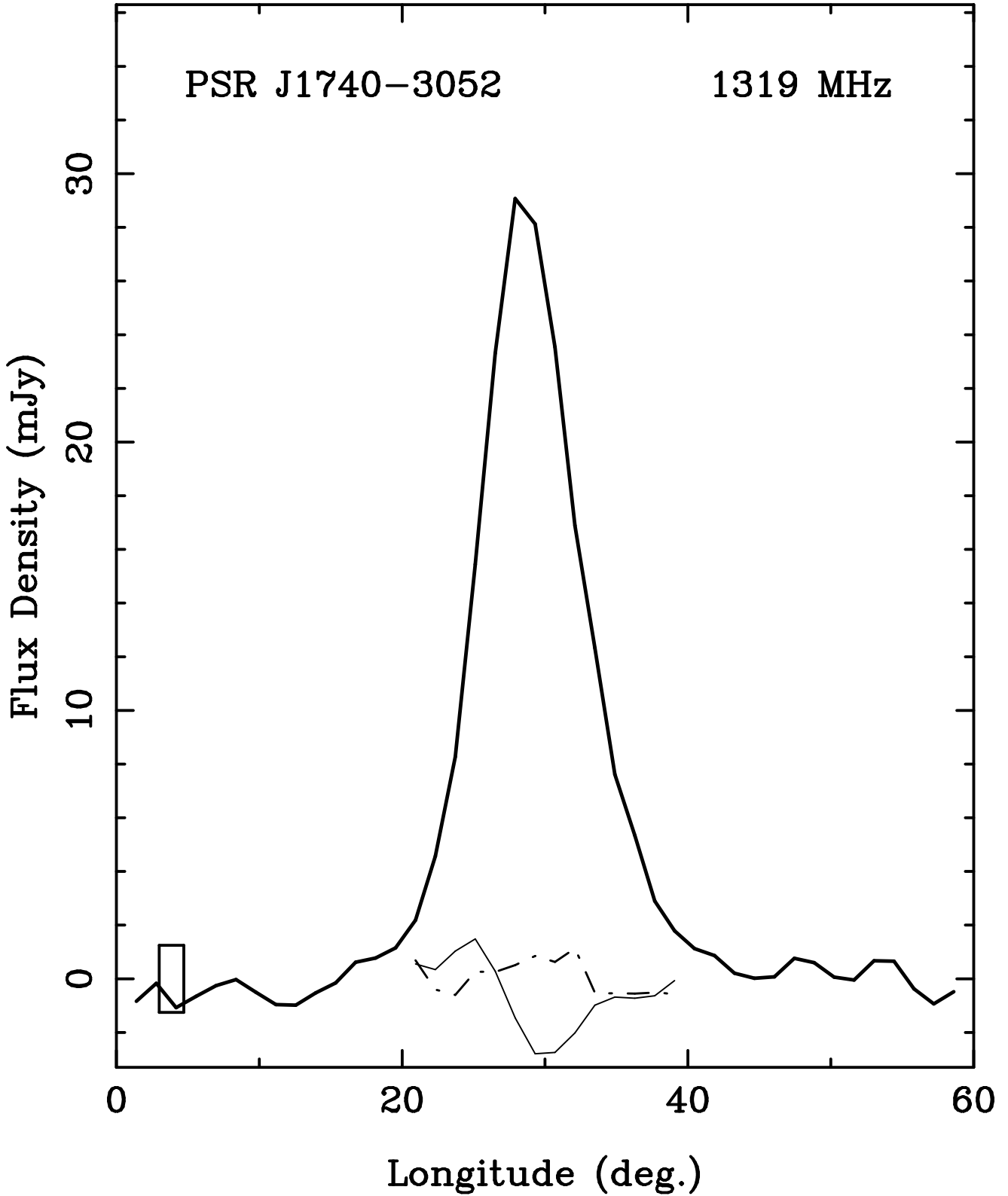


**Figure 7.** Mean pulse polarisation profile for PSR J1740–3052 obtained by summing 5.85 h of data obtained at 1318.5 MHz in 2000 February. The upper solid line is the total intensity, Stokes  $I$ , the dot-dashed line is the linearly polarised component,  $L = (Q^2 + U^2)^{1/2}$ , and the lower solid line is Stokes  $V = I_{LH} - I_{RH}$ . The box at the left of the baseline has a height of four times the baseline rms noise and a width equal to the effective time resolution of the profile, including the effects of interstellar dispersion. Position angles were not significant, and hence are not plotted.